

# Energy levels of mesonic helium in quantum electrodynamics

V. I. Korobov

*BLTP JINR, Dubna, Russia and*

*Samara National Research University, Samara, Russia*

A. V. Eskin, A. P. Martynenko, and F. A. Martynenko

*Samara National Research University, Samara, Russia*

On the basis of variational method we study energy levels of pionic helium ( $\pi - e - He$ ) and kaonic helium ( $K - e - He$ ) with an electron in ground state and a meson in excited state with principal and orbital quantum numbers  $n \sim l + 1 \sim 20$ . Variational wave functions are taken in the Gaussian form. Matrix elements of the basic Hamiltonian and corrections to vacuum polarization and relativism are calculated analytically in a closed form. We calculate some bound state energies and transition frequencies which can be studied in the experiment.

PACS numbers: 36.10.Gv, 12.20.Ds, 14.40.Aq, 12.40.Vv

Keywords: Kaonic helium, pionic helium, variational method, quantum electrodynamics

## I. INTRODUCTION

One of the directions in the development of the theory of fundamental interactions is connected with a study of bound states of particles. In addition to usual stable atoms and molecules that exist in our world, there are exotic bound states (muonium, positronium, positronium ion, muonic hydrogen, and others), which have attracted the attention of both experimenters and theoreticians for decades [1–3]. Although they have a short lifetime, nevertheless, by studying various energy intervals in the energy spectrum of such systems, as well as their decay widths, year after year it was possible to obtain from these studies more accurate information about the values of fundamental parameters of the Standard Model. A number of such exotic systems has been growing in recent years. For example, in [4, 5], it was proposed to study by laser spectroscopy method pionic helium atoms, which consist of a negative pion, an electron, and a helium nucleus. From a measurement of pion transitions between states with large values of the principal and orbital quantum numbers ( $(n, l) = (17.16) \rightarrow (17.15)$ ) one can try to obtain a more accurate value of the pion mass than can be done by other methods. In [6, 7], a successful experiment has already been carried out for nearly circular orbits  $n \sim l + 1$ , which gave a transition frequency value of 183760 MHz. To find a more accurate value of the pion mass from these measurements, it is also necessary to take into account systematic effects such as collision induced shift, broadening of the transition lines and others [8–10]. The work in this direction is in an active phase. Along with the atoms of pionic helium, other atoms can be proposed and studied, for example, kaonic helium, setting as the goal of research a more accurate determination of the mass of the  $K^-$  meson. It will be useful to note that there are other approaches to clarifying a value of the  $\pi$  meson mass. Thus, the study carried out in [11] demonstrates the potential of crystal spectroscopy of curved crystals in the field of exotic atoms. In this work,  $5g - 4f$

transitions in pionic nitrogen and muonic oxygen were measured simultaneously in a gaseous nitrogen-oxygen mixture. Knowing the muon mass, the muon line can be used to energy calibrate the pion transition. The mass value of negatively charged pion was obtained, which is 4.2 ppm higher than the current world average  $139.57077 \pm 0.00017$  MeV [12].

Mesonic atoms are formed as a result of a replacement of an orbital electron by a negatively charged meson. After that, laser spectroscopy of such atoms is carried out, which will make it possible to measure transition frequencies and determine the reduced mass of a system and hence a mass of the meson. To reduce the influence of strong interaction between a meson and a nucleus, the meson's orbit is raised by increasing its orbital momentum. The long lifetime of a meson atom is determined by the state with a large value of orbital momentum  $l = (16 \div 20)$  in which a meson is formed in the atom. Its transition to the ground state with  $l = 0$  is strongly suppressed. The lifetime of such an atom is several nanoseconds.

The study of energy levels of three-particle systems can be carried out with high accuracy within the framework of the variational method. There are some differences in the use of a variational method to find the energy levels of three-particle systems. They are connected with a choice of coordinates and representation of the Hamiltonian to describe the system, with a choice of basis wave functions. Thus, in [4] an exponential basis was used, and the coordinates of the electron and meson are determined with respect to the nucleus. In works [13–15], when calculating the energy levels of mesomolecules of hydrogen, muonic helium, etc., we use the Jacobi coordinates. The purpose of this work is to calculate the energy levels in pionic and kaonic helium atoms, as well as transition frequencies between levels in which the meson is in an excited state with a large orbital quantum number.

## II. GENERAL FORMALISM

Different approaches have been developed for a study of three-particle systems. There is an analytical method of perturbation theory, which makes it possible to analytically investigate both the Lamb shift and the hyperfine structure of the spectrum [15–21]. Another methods that are used for many-particle systems are the variational method and method of hyperspherical coordinates, which allow one to find energy levels and wave functions with very high accuracy [22–30]. Since for mesonic helium the states of an atom with large values of orbital moments of the meson are considered so that the electron and meson are at the same distance from the nucleus, it is virtually impossible to use a method of analytical perturbation theory. Therefore, further we study this system on the basis of the variational method. The Gaussian basis is used as the basis set of wave functions.

To find the energy levels of a three-particle system, we introduce the Jacobi coordinates  $\boldsymbol{\rho}$ ,  $\boldsymbol{\lambda}$ , which are related to the particle radius vectors  $\mathbf{r}_1$  (nucleus),  $\mathbf{r}_2$  (meson),  $\mathbf{r}_3$  (electron) as follows:

$$\boldsymbol{\rho} = \mathbf{r}_2 - \mathbf{r}_1, \quad \boldsymbol{\lambda} = \mathbf{r}_3 - \frac{m_1\mathbf{r}_1 + m_2\mathbf{r}_2}{m_1 + m_2}, \quad (1)$$

where  $m_1$ ,  $m_2$ ,  $m_3$  are the masses of  $He$  nucleus,  $\pi^-$  ( $K^-$ )-meson and electron.

To solve the variational problem, we choose the ground state trial basis wave functions in the form of superposition of the Gaussian exponents:

$$\Psi(\boldsymbol{\rho}, \boldsymbol{\lambda}, A) = \sum_{i=1}^K C_i \psi_i(\boldsymbol{\rho}, \boldsymbol{\lambda}, A^i), \quad \psi_i(\boldsymbol{\rho}, \boldsymbol{\lambda}, A^i) = e^{-\frac{1}{2}(A_{11}^i \boldsymbol{\rho}^2 + 2A_{12}^i \boldsymbol{\rho} \boldsymbol{\lambda} + A_{22}^i \boldsymbol{\lambda}^2)}, \quad (2)$$

where  $C_i$  are linear variational parameters,  $A^i$  is the matrix of nonlinear variational parameters,  $K$  is the basis size.

In nonrelativistic approximation the Hamiltonian of a three-particle atom in the Jacobi coordinates can be presented as

$$\hat{H}_0 = -\frac{1}{2\mu_1}\nabla_{\rho}^2 - \frac{1}{2\mu_2}\nabla_{\lambda}^2 + \frac{e_1e_2}{|\rho|} + \frac{e_1e_3}{|\lambda + \frac{m_2}{m_{12}}\rho|} + \frac{e_2e_3}{|\lambda - \frac{m_1}{m_{12}}\rho|}, \quad (3)$$

where  $m_{12} = m_1 + m_2$ ,  $\mu_1 = \frac{m_1m_2}{m_1+m_2}$ ,  $\mu_2 = \frac{(m_1+m_2)m_3}{m_1+m_2+m_3}$ ,  $e_1, e_2, e_3$  are the particle charges.

For arbitrary states of the meson and electron with orbital angular momenta  $l_1$  and  $l_2$ , a convenient basis for the expansion of functions depending on two directions are bipolar spherical harmonics [31]:

$$[Y_{l_1}(\theta_{\rho}, \phi_{\rho}) \otimes Y_{l_2}(\theta_{\lambda}, \phi_{\lambda})]_{LM} = \sum_{m_1, m_2} C_{l_1 m_1 l_2 m_2}^{LM} Y_{l_1 m_1}(\theta_{\rho}, \phi_{\rho}) Y_{l_2 m_2}(\theta_{\lambda}, \phi_{\lambda}), \quad (4)$$

where  $\theta_{\rho}, \phi_{\rho}$  and  $\theta_{\lambda}, \phi_{\lambda}$  are spherical angles that determine the direction of the vectors  $\rho, \lambda$ . Since the  $\pi^-$  or  $K^-$  meson are in an orbital excited state  $l$  in pionic (kaonic) helium, and the electron is in the ground state the variational wave function of the system is chosen for such states in the form:

$$\Psi_{lm}(\rho, \lambda, A) = \sum_{i=1}^K C_i Y_{lm}(\theta_{\rho}, \phi_{\rho}) \rho^l e^{-\frac{1}{2}(A_{11}^i \rho^2 + 2A_{12}^i \rho \lambda + A_{22}^i \lambda^2)}, \quad (5)$$

where spherical function  $Y_{lm}(\theta_{\rho}, \phi_{\rho})$  describes the angular part of the orbital motion of a pion (kaon).

Within the framework of the variational approach, the solution of the Schrödinger equation is reduced to solving the following matrix problem for the coefficients  $C_i$ :

$$H \cdot C = EB \cdot C, \quad (6)$$

where the matrix elements of the Hamiltonian  $H_{ij}$  and normalizations  $B_{ij}$  can be calculated analytically in a basis of the Gaussian wave functions. Thus, the normalization of the wave function (5) is determined by the following expression:

$$\langle \Psi | \Psi \rangle = \sum_{i,j=1}^K C_i C_j 2^{l+2} \pi^{3/2} \Gamma\left(l + \frac{3}{2}\right) \frac{B_{22}^l}{(\det B)^{l+\frac{3}{2}}}, \quad B_{kn} = A_{kn}^i + A_{kn}^j, \quad (7)$$

where  $\Gamma(l + 3/2)$  is the Euler gamma function.

Consider further analytical results for the matrix elements of the Hamiltonian. The kinetic energy operator contains two terms. The matrix element from the Laplace operator with respect to  $\lambda$  has the form:

$$\langle \Psi | \nabla_{\lambda}^2 | \Psi \rangle = \sum_{i,j=1}^K C_i C_j 2^{l+2} \pi^{\frac{3}{2}} \Gamma\left(l + \frac{3}{2}\right) \frac{B_{22}^{l-1}}{(\det B)^{l+\frac{5}{2}}} \times \quad (8)$$

$$[3A_{22}^i (A_{22}^i - B_{22}) \det B + (2l + 3)(A_{22}^i B_{12} - A_{12}^i B_{22})^2].$$

Similar matrix element with the Laplace operator in  $\rho$  is also expressed in terms of nonlinear variational parameters as follows:

$$\langle \Psi | \nabla_{\rho}^2 | \Psi \rangle = \sum_{i,j=1}^K C_i C_j 2^{l+1} \pi^{\frac{3}{2}} \Gamma \left( l + \frac{1}{2} \right) \frac{B_{22}^{l-1}}{(\det B)^{l+\frac{5}{2}}} \times \quad (9)$$

$$[(2l+1)\det B(-2l+3)A_{11}^i B_{22} + 3(A_{12}^i)^2 + 2lA_{12}^i B_{12}) + (2l+1)(2l+3)(A_{12}^i B_{12} - A_{11}^i B_{22})^2].$$

The potential energy operator in nonrelativistic Hamiltonian consists of pairwise Coulomb interactions  $U_{ij}$  ( $i, j=1, 2, 3$ ). The convenience of using the Gaussian basis in this case also lies in the possibility of analytical representation of the matrix elements of potential energy (in electronic atomic units):

$$\langle \Psi | U_{12} | \Psi \rangle = -Z \sum_{i,j=1}^K C_i C_j 2^{l+\frac{3}{2}} \pi^{\frac{3}{2}} \Gamma(l+1) \frac{B_{22}^{l-1}}{(\det B)^{l+1}}, \quad (10)$$

$$\langle \Psi | U_{13} | \Psi \rangle = -Z \sum_{i,j=1}^K C_i C_j 2^{l+\frac{5}{2}} \pi \Gamma \left( l + \frac{3}{2} \right) \frac{B_{22}^{l+\frac{1}{2}}}{(\det B)^{l+\frac{3}{2}}} {}_2F_1 \left( \frac{1}{2}, l + \frac{3}{2}, \frac{3}{2}, -\frac{(F_2^{23})^2}{\det B} \right) \quad (11)$$

$$\langle \Psi | U_{23} | \Psi \rangle = \sum_{i,j=1}^K C_i C_j 2^{l+\frac{5}{2}} \pi \Gamma \left( l + \frac{3}{2} \right) \frac{B_{22}^{l+\frac{1}{2}}}{(\det B)^{l+\frac{3}{2}}} {}_2F_1 \left( \frac{1}{2}, l + \frac{3}{2}, \frac{3}{2}, -\frac{(F_2^{13})^2}{\det B} \right) \quad (12)$$

$$F_2^{13} = B_{12} + \frac{m_1}{m_{12}} B_{22}, \quad F_2^{23} = B_{12} - \frac{m_2}{m_{12}} B_{22}, \quad (13)$$

where  ${}_2F_1(\alpha, \beta, x)$  is a hypergeometric function.

For  $l = 1$  the expressions (11)-(13) coincide with previously obtained results [32]. Using the matrix elements of the  $\hat{H}_0$  hamiltonian, some energy levels of the  $\pi^-$ -meson and  $K^-$ -meson atoms are calculated in Matlab system. The calculations are carried out using our program, which was previously used to calculate the energy levels of various muonic atoms in quantum electrodynamics. The calculation of the energy levels of the  $\pi^-$ -meson atom is carried out in order to test the operation of the program. The calculation results are shown in Table I.

To improve the accuracy of the calculation, we consider some important corrections to the Hamiltonian  $\hat{H}_0$ . The pair electromagnetic interaction between particles in quantum electrodynamics is determined by the Breit potential [33]. Among the various terms in this potential, let us single out those terms that have the greatest numerical value. These include relativistic corrections, contact interaction and corrections for vacuum polarization.

The relativistic corrections are defined in the energy spectrum by the following terms in electronic atomic units:

$$\Delta U_{rel} = -\frac{\alpha^2}{8} \left( \frac{\mathbf{p}_1^4}{m_1^3} + \frac{\mathbf{p}_2^4}{m_2^3} + \frac{\mathbf{p}_3^4}{m_3^3} \right). \quad (14)$$

The term of leading order in (14) is related with a motion of the electron. The value of the matrix element from  $\Delta U_{rel}^e$  can be obtained in exactly the same way as (8) in terms of variational parameters:

$$\langle \Psi | -\frac{\alpha^2}{8} \nabla_{\lambda}^4 | \Psi \rangle = -\frac{\alpha^2}{8} \sum_{i,j=1}^K C_i C_j 2^{l+1} \pi^{\frac{1}{2}} \Gamma \left( l + \frac{3}{2} \right) \frac{B_{22}^{l-2}}{(\det B)^{l+\frac{7}{2}}} \left[ 15(A_{22}^i)^2 (\det B)^2 (A_{22}^i - B_{22})^2 + \right. \quad (15)$$

$$10(2l+3)A_{22}^i(A_{22}^i - B_{22})\det B(A_{22}^i B_{12} - A_{12}^i B_{22})^2 + (2l+3)(2l+5)(A_{22}^i B_{12} - A_{12}^i B_{22})^4].$$

TABLE I: Energy levels of the meson atom obtained in nonrelativistic approximation with the Gaussian and exponential basis and values of main corrections in the energy spectrum in electron atomic units (e.a.u.).

State	$E_{nr}(\text{Exp})$	$E_{nr}(\text{G})$	$-\frac{\alpha^2}{8}\mathbf{p}_e^4$	$\Delta U_{vp}$	$\Delta U_{cont}$
$({}^3_2\text{He} - \pi^- - e)$ atom					
(17,16)	-2.64312261030188(2)[4]	-2.6423822152	-0.0000568853	-0.0000003596	0.0000021185
(17,15)	-2.6709980910(1)[4]	-2.6698284795	-0.0000578381	-0.0000003646	0.0000021477
$({}^4_2\text{He} - \pi^- - e)$ atom					
(17,16)	-2.65751243850171[4]	-2.6567689659	-0.0000560957	-0.0000003549	0.0000020904
(17,15)	-2.68542722(2)[4]	-2.6842422023	-0.0000571739	-0.0000003606	0.0000021242
$({}^3_2\text{He} - K^- - e)$ atom					
(20,19)	-4.6685977528	-4.6806222136	-0.0000194273	-0.0000001272	0.0000007495
(20,18)	-4.6786693864	-4.6932218265	-0.0000178752	-0.0000001159	0.0000006829
(21,20)	-4.3199030879	-4.3133610685	-0.0000238657	-0.0000001466	0.0000008638
(21,19)	-4.3285605454	-4.3238629798	-0.0000230792	-0.0000001498	0.0000008827
$({}^4_2\text{He} - K^- - e)$ atom					
(20,19)	-4.8266672526	-4.8328936568	-0.0000190789	-0.0000001231	0.0000007252
(20,18)	-4.8520548999	-4.8578478878	-0.0000172623	-0.0000001161	0.0000006552
(21,20)	-4.4573174498	-4.4499843007	-0.0000207687	-0.0000001490	0.0000008777
(21,19)	-4.4653630953	-4.4601685694	-0.0000219706	-0.0000001409	0.0000008299

Let us also take into account the vacuum polarization effects in the energy spectrum. Since for both an electron and a meson in a highly excited state, the Compton wavelength of an electron is much smaller than the radius of the Bohr orbit, we can use the following expression for the vacuum polarization potential in electronic atomic units:

$$\Delta U_{vp} = \Delta U_{vp}(r_{13}) + \Delta U_{vp}(r_{23}) = -\frac{4}{15}\alpha^2(Z\alpha)\delta(\boldsymbol{\lambda} + \frac{m_2}{m_{12}}\boldsymbol{\rho}) + \frac{4}{15}\alpha^2(Z\alpha)\delta(\boldsymbol{\lambda} - \frac{m_1}{m_{12}}\boldsymbol{\rho}). \quad (16)$$

The matrix elements of such potentials are calculated analytically in a closed form:

$$\langle \Psi | \Delta U_{vp}(r_{13}) | \Psi \rangle = -\frac{4}{15}\alpha^2(Z\alpha) \sum_{i,j=1}^K C_i C_j 2^{l+\frac{1}{2}} \Gamma\left(l + \frac{3}{2}\right) \frac{1}{(F_1^{13})^{l+\frac{3}{2}}}, \quad (17)$$

$$\langle \Psi | \Delta U_{vp}(r_{23}) | \Psi \rangle = -\frac{4}{15}\alpha^2(Z\alpha) \sum_{i,j=1}^K C_i C_j 2^{l+\frac{1}{2}} \Gamma\left(l + \frac{3}{2}\right) \frac{1}{(F_1^{23})^{l+\frac{3}{2}}}, \quad (18)$$

$$F_1^{13} = B_{11} + \frac{m_2^2}{m_{12}^2} B_{22} - 2\frac{m_2}{m_{12}} B_{12}, \quad F_1^{23} = B_{11} + \frac{m_1^2}{m_{12}^2} B_{22} + 2\frac{m_1}{m_{12}} B_{12}. \quad (19)$$

The contact interaction potential, as well as (16), is expressed through the  $\delta$ -functions in the form (in electronic atomic units):

$$\Delta U_{cont} = \frac{\pi Z \alpha^2}{2} \delta(\boldsymbol{\lambda} + \frac{m_2}{m_{12}} \boldsymbol{\rho}) - \frac{\pi \alpha^2}{2} \delta(\boldsymbol{\lambda} - \frac{m_1}{m_{12}} \boldsymbol{\rho}). \quad (20)$$

In Table I we present the results of calculating the energy values with the Hamiltonian  $\hat{H}_0$  and the values of the matrix elements (15), (17), (18). (20).

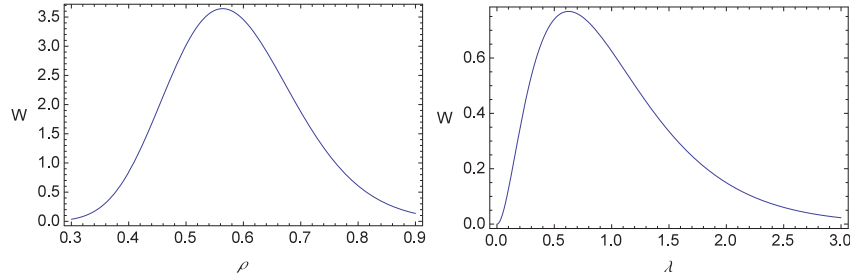


FIG. 1: The radial distribution densities  $W(\rho)$ ,  $W(\lambda)$  for  $({}^3_2He - \pi^- - e)$  for the state (16, 15). The variable values  $\rho$  and  $\lambda$  are taken in electron atomic units.

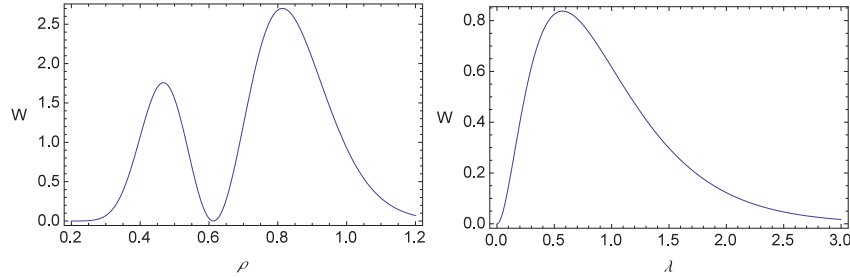


FIG. 2: The radial distribution densities  $W(\rho)$ ,  $W(\lambda)$  for  $({}^3_2He - \pi^- - e)$  for the state (17, 15). The variable values  $\rho$  and  $\lambda$  are taken in electron atomic units.

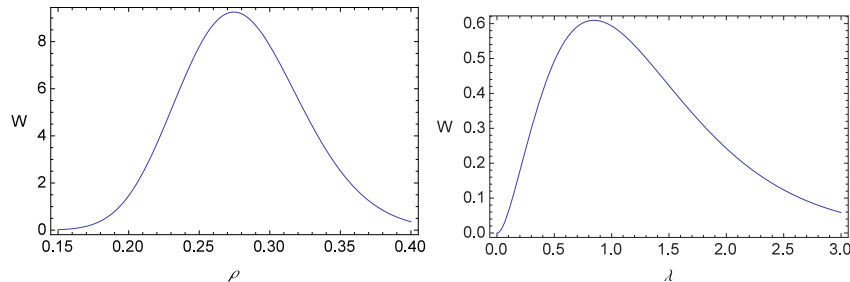


FIG. 3: The radial distribution densities  $W(\rho)$ ,  $W(\lambda)$  for  $({}^3_2He - K^- - e)$  for the state (21, 20). The variable values  $\rho$  and  $\lambda$  are taken in electron atomic units.

The obtained wave functions (5) make it possible to calculate the radial distribution densities in  $\rho$  and  $\lambda$  and root mean square values  $\sqrt{\langle \rho^2 \rangle}$ ,  $\sqrt{\langle \lambda^2 \rangle}$ , which are determined

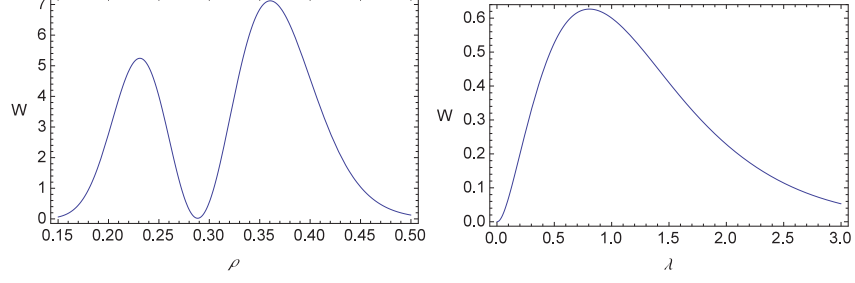


FIG. 4: The radial distribution densities  $W(\rho)$ ,  $W(\lambda)$  for  $({}^3\text{He} - K^- - e)$  for the state (22, 20). The variable values  $\rho$  and  $\lambda$  are taken in electron atomic units.

by the expressions:

$$W(\rho) = \frac{(2\pi)^{3/2}}{\langle \Psi | \Psi \rangle} \sum_{i,j=1}^K \frac{C_i C_j}{B_{22}^{3/2}} \rho^{(2l+2)} e^{-\frac{1}{2} \frac{\det B}{B_{22}} \rho^2}, \quad (21)$$

$$W(\lambda) = \frac{2^{l+\frac{5}{3}} \pi}{\langle \Psi | \Psi \rangle} \sum_{i,j=1}^K \frac{C_i C_j \Gamma(l + \frac{3}{2})}{B_{11}^{l+\frac{3}{2}}} \lambda^2 e^{-\frac{1}{2} B_{22} \lambda^2} {}_1F_1\left(l + \frac{3}{2}, \frac{3}{2}, \frac{B_{12}^2 \lambda^2}{2B_{11}}\right), \quad (22)$$

$$W(\rho, \lambda) = \frac{4\pi}{\langle \Psi | \Psi \rangle} \sum_{i,j=1}^K \frac{C_i C_j}{B_{12}} \rho^{2l+1} \lambda e^{-\frac{1}{2} [B_{11} \rho^2 + B_{22} \lambda^2]} \text{sh}(B_{12} \rho \lambda), \quad B_{lk} = A_{lk}^i + A_{lk}^j, \quad (23)$$

$$\langle \rho^2 \rangle = \frac{\pi^{\frac{3}{2}} 2^{l+3} \Gamma(l + \frac{5}{2})}{\langle \Psi | \Psi \rangle} \sum_{i,j=1}^K C_i C_j \frac{B_{22}^{l+1}}{(\det B)^{l+5/2}}, \quad (24)$$

$$\langle \lambda^2 \rangle = \frac{\pi^{\frac{3}{2}} 2^{l+2} \Gamma(l + \frac{3}{2})}{\langle \Psi | \Psi \rangle} \sum_{i,j=1}^K C_i C_j \frac{B_{22}^{l-1}}{(\det B)^{l+5/2}} (3B_{11} B_{22} + 2B_{12}^2 l). \quad (25)$$

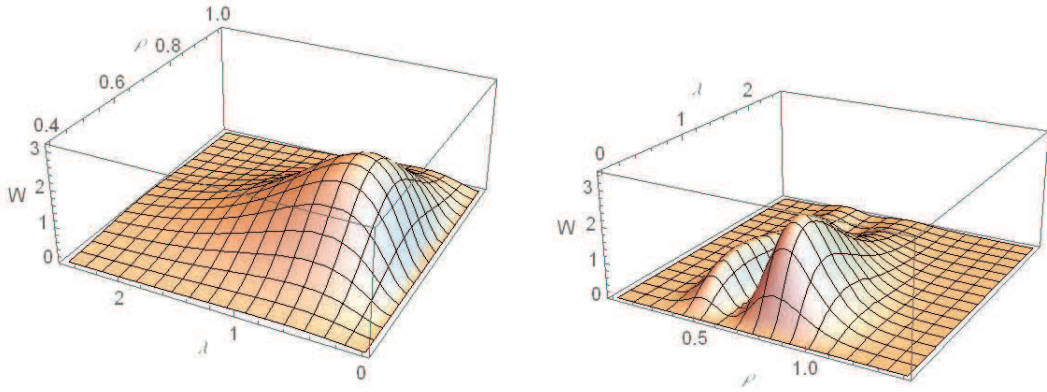


FIG. 5: The radial distribution density  $W(\rho, \lambda)$  for  $(\pi e^4 \text{He})$  in states (17,16) and (17,15). The variable values  $\rho$  and  $\lambda$  are taken in electron atomic units.

The radial distribution densities are presented in Fig. 1, 2 in the case of pionic helium and kaonic helium. These plots show the presence of characteristic distances in the particle systems  $(\text{He} - \pi^- - e)$  and  $(\text{He} - K^- - e)$ . It also follows from these graphs that for the

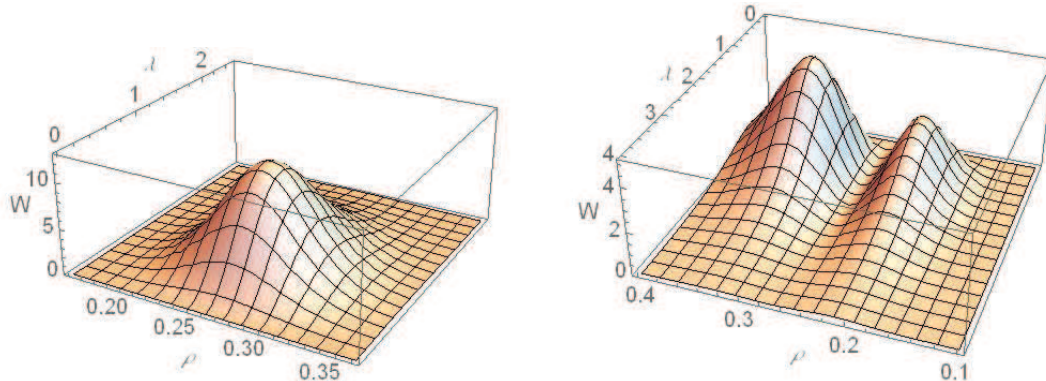


FIG. 6: The radial distribution density  $W(\rho, \lambda)$  for  $(Ke^3He)$  in states  $(21,20)$  and  $(21,19)$ . The variable values  $\rho$  and  $\lambda$  are taken in electron atomic units.

considered states, the meson turns out to be located at the same distances from the nucleus or slightly closer to the nucleus than the electron. The distribution densities for the two radial variables  $\rho$  and  $\lambda$  provide a more complete picture of the characteristic distances in a given system of three particles. They are shown in two graphs in Fig. 5,6.

Fine splitting in a three-particle atom which is determined by the interaction of the electron spin and the large orbital angular momentum of the meson is not considered here.

### III. DISCUSSION OF THE RESULTS

This paper examines the energy levels of pionic and kaonic helium for states in which the meson has such a large orbital momentum that it is located approximately at the same distance from the nucleus as the electron. The calculations are performed in leading order within the framework of the variational method with the Gaussian basis, and a number of basic corrections determined by the Breit Hamiltonian (for relativism, vacuum polarization and contact interaction) are calculated in the first order of perturbation theory. Since an electron is in the  $1S$  state, the notation  $(n, l)$  is used for a state of three particles in Table I, where  $l$  is the orbital momentum of the meson, and  $n$  is the principal quantum number for the subsystem  $(\pi^- He^{2+})$ ,  $(K^- He^{2+})$ .

The Rydberg states in atoms play an important role in refining the values of fundamental constants. Thus, based on the spectroscopy of the Rydberg states in a hydrogen atom, the measurement of the Rydberg constant has been improved [34, 35]. In this problem, by working with the Rydberg states, it is possible to eliminate contributions to the structure of a nucleus. In the case of mesonic atoms, a use of the Rydberg states makes it possible to reduce the influence of strong interaction on the energy spectrum.

Spectroscopy of various exotic molecules can provide new information about a nature of fundamental interactions and the values of fundamental parameters of the Standard Model. Several years ago, the PiHe collaboration at the Paul Scherrer Institute performed laser spectroscopy of the infrared transition in three-body pion helium atoms [4, 5]. Such atoms were created in a superfluid (He-II) helium target. Similar measurements in antiproton helium atoms embedded in liquid helium were carried out by the CERN ASACUSA collaboration [36]. The antiproton-to-electron mass ratio was determined as  $m_p/m_e=1836.1526734(15)$  [36]. The mass of  $\pi$  meson can be determined by comparing the experimental transition fre-



quencies in pionic helium with results of the QED calculation [4]. Although the transition frequency  $(17, 16) \rightarrow (17, 15)$  has already been measured for pionic helium [5], an analysis of experimental data to extract the pion mass is still ongoing.

Our study of the energy levels of both pionic and kaonic helium is carried out on the basis of the variational approach, which was developed in the work [28]. In contrast to the work [4], to describe a three-particle system, the Jacobi coordinates  $\rho, \lambda$  are used, in which the original Hamiltonian has the form (3). The second difference between our calculation and [4] is the use of a Gaussian rather than an exponential basis within the variational method. In such a basis, all matrix elements of the Hamiltonian are obtained in a closed analytical form. Finally, the third difference between our calculations and [4] is that in [4], within the framework of the variational approach, the method of complex coordinate rotation is used, and we work with a real Hamiltonian and solve the eigenvalue problem (6). The obtained numerical results for leading order contribution to the energy of a system and corrections to it are presented in Table I. Comparing these results with calculation in [4], it is necessary to note a slight difference in the results, which appears in the third digit after the decimal point (second coulomb in Table I). For the  $(17,16) \rightarrow (17,15)$  transition frequency for pionic helium-4 that has been measured, our result 180772 GHz is slightly different (near one per cent) from the result  $183681.5 \pm 0.5$  GHz obtained in [4] and from experimental value, which is 183760(6)(6) GHz. Our result for similar transition frequency in pionic helium-3 is equal 180594 GHz. We also present here the results for the transition frequencies  $(21, 20) \rightarrow (21, 19)$  in the case of kaonic helium. They are equal 69094 GHz ( $K - e - \frac{3}{2}He$ ) and 67017 GHz ( $K - e - \frac{4}{2}He$ ). In general, our results using the Gaussian trial functions (third column of Table I) are consistent with calculations with an exponential basis in [4] (second column of Table I) in the case of pionic helium. In the case of kaonic helium the obtained results are new. The difference in results is due, in our opinion, to differences in the used variational approaches in this work and in [4] and bases for variational wave functions.

A study of characteristic distances at which the nucleus, meson and electron are located relative to each other is shown in Figs. 1-6 for some states for which the binding energies are calculated. The meson is in an excited state with a large orbital momentum  $l$ . The key parameter with which you can estimate its distance to the nucleus is determined by the expression  $\sqrt{\mu_1/m_3}$ , where  $\mu_1$  is the reduced mass of the meson-nucleus system and  $m_3$  is the electron mass. When the principal quantum number  $n = \sqrt{\mu_1/m_3} \approx 16$  for the  $(\pi^{-4}He)$  or  $(\pi^{-3}He)$  subsystems, a movement of the  $\pi^-$ -meson occurs at approximately the same distances from the nucleus and with the same binding energy as for an electron. In the case of kaonic helium, the value of the principal quantum number increases due to an increase in the meson mass and reaches the value  $n \approx 29$ . This parameter determines the order of the principal quantum number  $n$ , at which the meson and electron have close orbits. But in this work we have so far considered slightly smaller values  $n \approx 20$ , so that the  $K^-$ -meson is located a little closer to the nucleus. It follows from Figs. 1-6 that in a case of the considered Rydberg states of the  $\pi^-$  ( $K^-$ )-meson, characteristic distances along  $\rho$  and  $\lambda$  have close values. So, for example, the root mean square value of  $\sqrt{\lambda^2}$  for the state  $(17,16)$  in  $(\pi - e - \frac{4}{2}He)$  is 60050 fm, and the root mean square value of  $\sqrt{\rho^2}$  for the same state is equal 37210 fm. This means that the use of an analytical method for calculating energy levels as in [13, 21] is difficult, since the characteristic series for the parameter  $M_e/M_\mu$  from [13, 21] is not rapidly converging.

When calculating relativistic effects, we take into account only corresponding correction for the electron, meaning that the electron is lightest particle in this system, and with an

increase in the principal quantum number  $n$ , the orbital speed is determined by the formula  $v = Z\alpha/n$ . Therefore, for a meson in the circular Rydberg states it is suppressed by the factor  $n$ .

In Table I we limited ourselves to presenting numerical results of calculating the energies of bound states of three particles only for a certain number of states with  $(n, l)$ . But obtained general analytical formulas for the matrix elements of the Hamiltonian of a system make it possible to carry out corresponding numerical calculations for other states  $(n, l)$ , which may be more important for the experiment. For the principal quantum number  $n = 29$ , the binding energy of kaonic helium in the state  $(n, l) = (29, 28)$  is equal to  $-2.8001942461$  e.a.u., and in the state  $(n, l) = (29, 27)$  it has the value  $-2.9152046696$  e.a.u., which ultimately gives the transition frequency between these levels  $\nu = 756732$  GHz.

### Acknowledgments

This work is supported by Russian Science Foundation (grant No. RSF 23-22-00143).

- 
- [1] M. I. Eides, H. Grotch and V. A. Shelyuto, Theory of light hydrogenlike atoms, Phys. Rept. **342**, 63 (2001).
  - [2] A. Antognini, F. Hagelstein, V. Pascalutsa, The proton structure in and out of muonic hydrogen, Ann. Rev. Nucl. Part. Sci. **72**, 389 (2022).
  - [3] C. Pizzolotto, A. Adamczak, D. Bakalov, G. Baldazzi, M. Baruzzo, The FAMU experiment: muonic hydrogen high precision spectroscopy studies, Eur. Phys. J. A **56**, 7, 185 (2020).
  - [4] M. Hori, A. Soter, V. I. Korobov, Proposed method for laser spectroscopy of pionic helium atoms to determine the charged-pion mass, Phys. Rev. A **89**, 042515 (2014).
  - [5] M. Hori, A. Soter, H. Aghai-Khozani, D. Barna, A. Dax et al., Method for laser spectroscopy of metastable pionic helium atoms, Hyperfine Interact. **234**, 1-3, 85 (2015).
  - [6] M. Hori, H. Aghai-Khozani, A. Soter, A. Dax, D. Barna, Laser spectroscopy of pionic helium atoms, Nature **581**, 37 (2020).
  - [7] M. Hori, H. Aghai-Khozani, A. Sótér, A. Dax, D. Barna, and L. Venturelli, Laser spectroscopy of long-lived pionic and antiprotonic helium in superfluid helium, PoS ICHEP2022 141.
  - [8] D. Bakalov, Calculation of the density shift and broadening of the transition lines in pionic helium: Computational problems, Hyperfine Interact. **233**, 1-3, 127-130 (2015).
  - [9] B. Obreshkov, Systematic Effects in the Measurement of the Negatively Charged Pion Mass Using Laser Spectroscopy of Pionic Helium Atoms, Nuclear Theory, Vol. 35 (2016), eds. M. Gaidarov, N. Minkov, Heron Press, Sofia.
  - [10] D. Bakalov and B. Obreshkov, Collisional shift and broadening of the transition lines in pionic helium, Phys. Rev. **93**, 062505 (2016).
  - [11] M. Trassinelli, D. F. Anagnostopoulos, G. Borchert et al., Measurement of the charged pion mass using X-ray spectroscopy of exotic atoms, Phys. Lett. B **759**, 583 (2016).
  - [12] R. L. Workman et al. (Particle Data Group), The Review of Particle Physics, Prog. Theor. Exp. Phys. 2022, 083C01 (2022).
  - [13] A. V. Eskin, V. I. Korobov, A. P. Martynenko and F. A. Martynenko, Energy Levels of Three-Particle Muon Electron Helium in Variational Approach, Phys. Atom. Nucl. **86**, 4, 583 (2023).

- [14] V. I. Korobov, A. P. Martynenko and F. A. Martynenko, A. V. Eskin, Muon Lamb Shift in Three-Particle Muon Electron Systems in Quantum Electrodynamics, Bull. Lebedev Phys. Inst., **50**, 6, 229 (2023).
- [15] A. V. Eskin, V. I. Korobov, A. P. Martynenko, F. A. Martynenko, Three Particle Muon Electron Bound Systems in Quantum Electrodynamics, Atoms **11**, 25 (2023).
- [16] S. D. Lakdawala and P. Mohr, Hyperfine structure in muonic helium, Phys. Rev. A **22**, 1572 (1980).
- [17] K. N. Huang and V. W. Hughes, Theoretical hyperfine structure of the muonic  ${}^3\text{He}$  and  ${}^4\text{He}$  atoms, Phys. Rev. A **26**, 2330 (1982).
- [18] M. Ya. Amusia, M. Ju. Kuchiev, V. L. Yakhontov, Computation of the hyperfine structure in the  $(\alpha - \mu^- - e^-)^0$  atom, J. Phys. B **16**, L71 (1983).
- [19] S. G. Karshenboim, V. G. Ivanov, M. Ya. Amusia, Lamb shift of electronic states in neutral muonic helium, an electron-muon-nucleus system, Phys. Rev. A **91**, 3, 032510 (2015).
- [20] A. A. Krutov and A. P. Martynenko, Ground-state hyperfine structure of the muonic helium atom, Phys. Rev. A **78**, 032513 (2008).
- [21] R. N. Faustov, V. I. Korobov, A. P. Martynenko, F. A. Martynenko, Ground-state hyperfine structure of light muon-electron ions, Phys. Rev. A **105**, 042816 (2022).
- [22] R. J. Drachman, Nonrelativistic hyperfine splitting in muonic helium by adiabatic perturbation theory, Phys. Rev. A **22**, 1755 (1980).
- [23] S. I. Vinitzky, V. S. Melezhik, I. I. Ponomarev et al., Calculation of Energy Levels of Hydrogen Isotope  $\mu$  Mesic Molecules in the Adiabatic Representation of Three-body Problem, Sov. Phys. JETP **52**, 353 (1980).
- [24] A. M. Frolov, Properties and hyperfine structure of helium-muonic atoms, Phys. Rev. A **61**, 022509 (2000).
- [25] A. M. Frolov, The hyperfine structure of the ground states in the helium-muonic atoms, Phys. Lett. A **376**, 2548 (2012).
- [26] M.-K. Chen, Correlated wave functions and hyperfine splitting of the 2s state of muonic  ${}^{3,4}\text{He}$  atoms, Phys. Rev. A **45**, 3, 1479 (1992).
- [27] H. Fatehizadeh, R. Gheisari, H. Falinejad, Full calculation of  $\mu\text{pd}$  and  $\mu\text{dt}$  muonic bound levels: Combination of Nikiforov-Uvarov method and variational approach, Ann. Phys. **385**, 512 (2017)
- [28] K. Varga and Y. Suzuki, Solution of few-body problems with the stochastic variational method I. Central forces with zero orbital momentum, Comp. Phys. Comm. **106**, 157 (1997).
- [29] V. I. Korobov, Variational Methods in the Quantum Three-Body Problem with Coulomb Interaction, Phys. Part. Nucl. **53**, No. 1, 5 (2022).
- [30] Md. A. Khan, Hyperspherical three-body calculation for exotic atoms, Few-Body Syst. **52**: 53-63 (2012).
- [31] D. A. Varshalovich, V. K. Khersonsky, E. V. Orlenko, and A. N. Moskalev, Quantum theory of angular momentum and its applications, V.1, M., Fizmatlit, 2017.
- [32] A. P. Martynenko, F. A. Martynenko, V. V. Sorokin, O. S. Sukhorukova, A. V. Eskin, Energy Levels of Mesomolecular Ions of Hydrogen in Variational Approach, Bull. Lebedev Phys. Inst. **46**, 4, 143 (2019).
- [33] L. D. Landau and E. M. Lifshitz, Course of Theoretical Physics, Vol. 4: Quantum Electrodynamics, Fizmatlit, M., 2008; Pergamon, NY, 1977, 3rd ed.
- [34] B. de Beauvoir, F. Nez, L. Julien, et al., Absolute Frequency Measurement of the 2S-8S/D Transitions in Hydrogen and Deuterium: New Determination of the Rydberg Constant, Phys.

- Rev. Lett. **78**, 440 (1997).
- [35] C. Schwob, L. Jozefowski, B. de Beauvoir, et al., Optical Frequency Measurement of the 2S-12D Transitions in Hydrogen and Deuterium: Rydberg Constant and Lamb Shift Determinations, Phys. Rev. Lett. **82**, 4960 (1999).
- [36] A. Sóter, H. Aghai-Khozani, D. Barna, A. Dax, L. Venturelli and M. Hori, High-resolution laser resonances of antiprotonic helium in superfluid  $^4\text{He}$ , Nature **603**, 411 (2022).